Available online at www.sciencedirect.com
SCIENCE DIRECT®
Journal of Luminescence 116 (2006) 145–150
JOURNAL OF LUMINESCENCE
www.elsevier.com/locate/jlumin

# Stark components of lower-lying manifolds and emission cross-sections of intermanifold and inter-stark transitions of $Nd^{3+}(4f^3)$ in polycrystalline ceramic garnet $Y_3Al_5O_{12}$

Dhiraj K. Sardar[a,*], Raylon M. Yow[a], John B. Gruber[b], Toomas H. Allik[c], Bahram Zandi[d]

[a]*Department of Physics and Astronomy, University of Texas at San Antonio, San Antonio, TX 78249-0697, USA*
[b]*Department of Physics, San José State University, San José, CA 95192-0106, USA*
[c]*Scientific Applications International Corporation, P.O. Box 632, Fort Belvoir, VA 22060-5806, USA*
[d]*ARL/Adelphi Mill Road, Adelphi, MD 20783-1197, USA*

Received 24 March 2005
Available online 16 September 2005

**Abstract**

Stark energy levels of the $^4F_{3/2}$, $^4I_{9/2}$, and $^4I_{11/2}$ manifolds have been characterized using the room temperature fluorescence spectra for the $^4F_{3/2}\rightarrow{}^4I_{9/2}$ and $^4F_{3/2}\rightarrow{}^4I_{11/2}$ transitions of $Nd^{3+}(4f^3)$ in polycrystalline ceramic garnet $Y_3Al_5O_{12}$ (YAG). The emission cross-sections of the intermanifold transitions, $^4F_{3/2}\rightarrow{}^4I_{9/2}$ and $^4F_{3/2}\rightarrow{}^4I_{11/2}$, as well as the principal inter-Stark transitions, $R_1\rightarrow Z_5$ (945.3 nm) and $R_1\rightarrow Y_2$ (1063.5 nm), have also been determined. These results are finally compared with those of $Nd^{3+}$:YAG single crystal.


*Keywords:* Stark energy levels; Emission cross-section; Polycrystalline ceramic garnet

## 1. Introduction

The ceramic $Nd^{3+}$:$Y_3Al_5O_{12}$ (YAG) has drawn a considerable interest due to its excellent spectroscopic and laser properties [1–5]. In a recent article, Kumar and co-workers have reported that because of its low pore volume and narrow grain boundary, ceramic $Nd^{3+}$:YAG has optical and stimulated emission properties that are similar to those of single-crystal $Nd^{3+}$:YAG [6]. In addition, they have demonstrated laser oscillations at 1.06 and 1.3 μm with slope efficiencies of 40% and 35%, respectively, suggesting that ceramic $Nd^{3+}$:YAG is a potential contender for the near infrared laser system. Sekita et al. have demonstrated that the optical properties of YAG

*Corresponding author. Tel.: +1 2104585748; fax: +1 2104584919.
*E-mail address:* dsardar@utsa.edu (D.K. Sardar).

0022-2313/$ - see front matter © 2005 Elsevier B.V. All rights reserved.
doi:10.1016/j.jlumin.2005.08.003

ceramics prepared by the urea precipitation method are similar to those of YAG single crystals grown by Czechralski and float zone methods [1]. Strong optical absorption of this material at 809 nm is particularly important for efficient pumping by the currently available powerful diode lasers. The radiative lifetime of the upper $^4F_{3/2}$ manifold and the branching ratios between the upper manifold and the corresponding lower multiplet manifolds have been predicted by the Judd–Ofelt (J–O) theory [6,7]. The room temperature fluorescence lifetime of the $Nd^{3+}$ $^4F_{3/2}$ level has been measured approximately 245 μs [7]. The long fluorescence lifetime is adequate for many applications which require higher energy storage. The branching ratio of the $^4F_{3/2} \rightarrow {}^4I_{11/2}$ transition has been found to be 51% compared to 38% for the $^4F_{3/2} \rightarrow {}^4I_{9/2}$ transition [7]. Owing to the higher energy storage capability and the larger branching ratio of the $^4F_{3/2} \rightarrow {}^4I_{11/2}$ transition, ceramic $Nd^{3+}$:YAG can be an excellent candidate for a 1.06 μm, Q-switched laser system which can be efficiently pumped by the high power laser diodes or tunable solid state lasers that have become more readily available.

In this article, we report a room temperature characterization of the Stark energy levels of the lower level manifolds $^4F_{3/2}$, $^4I_{9/2}$, and $^4I_{11/2}$. We have also determined the emission cross-sections of the $^4F_{3/2} \rightarrow {}^4I_{9/2}$ and $^4F_{3/2} \rightarrow {}^4I_{11/2}$ intermanifold transitions as well as the principal inter-Stark peak transitions at $R_1 \rightarrow Z_5$ (945.3) and $R_1 \rightarrow Y_2$ (1063.5 nm) within the respective intermanifold multiplets using the room temperature emission spectra of $Nd^{3+}$ in ceramic YAG host. The spectroscopic parameters of ceramic $Nd^{3+}$:YAG are then compared with those of single-crystal $Nd^{3+}$:YAG.

## 2. Experimental method

A spectroscopic sample of polycrystalline ceramic $Nd^{3+}$:YAG was obtained from Baikowski International Corporation, Charlotte, NC [8]. The sample disc was 7.21 mm in diameter and 1.71 mm thick. The $Nd^{3+}$ concentration was found to be $1.87 \times 10^{20}\,cm^{-3}$. The room temperature fluorescence spectra were measured on ceramic $Nd^{3+}$:YAG by exciting the sample at 514.5 nm from a Spectra Physics model 2005 argon ion laser. The laser beam was focused in about 1.0 mm diameter spot on to the sample with the help of a positive lens. The maximum laser power used in all the measurements was 1.5 W. The emission from the sample was collected by a pair of positive lenses at 90° with respect to the exciting laser beam, and detected by a liquid nitrogen-cooled Ge detector attached to the exit slit of a SPEX model 340E monochromator. A Hoya sharp-cut filter O-54 was used at the entrance slit of the monochromator to prevent the exciting laser beam from entering the monochromator. The monochromator was equipped with a reflection grating with 600 grooves/mm and blazed at 1.0 μm. The spectral resolution in all of our measurements was better than 0.8 nm. The signal was then taken from the detector to a Spex Datascan model DS 1000 equipped with a RS-232 interface card. A computer was used to control the monochromator and to acquire and analyze the data.

## 3. Results and discussion

The J–O model was applied to the room temperature absorption spectrum of ceramic $Nd^{3+}$:YAG to determine the J–O intensity parameters, that were subsequently utilized to determine the radiative decay rates, branching ratios of $Nd^{3+}$ transitions from the $^4F_{3/2}$ manifold to the $^4I_J$ lower-lying manifolds, and the radiative lifetime of the $^4F_{3/2}$ metastable manifold [7]. The fluorescence lifetime of the $^4F_{3/2} \rightarrow {}^4I_{11/2}$ transition was measured at room temperature and compared with the radiative lifetime to determine quantum efficiency [7]. These spectroscopic parameters of ceramic $Nd^{3+}$:YAG are compared with those reported by Kumar et al. [6] and also those of single-crystal $Nd^{3+}$:YAG in Table 1.

The room temperature emission spectra for the $^4F_{3/2} \rightarrow {}^4I_{9/2}$ and $^4F_{3/2} \rightarrow {}^4I_{11/2}$ transitions of $Nd^{3+}(4f^3)$ in polycrystalline ceramic YAG are given in Figs. 1 and 2, respectively. The $^4F_{3/2} \rightarrow {}^4I_{11/2}$ transition stands out as the strongest

Table 1
Spectroscopic properties of 1.0 at% $Nd^{3+}(4f^3)$ doped in ceramic and single crystal (sc) YAG

| Parameters | | Nd:YAG (ceramic)[a] | Nd:YAG (ceramic) [6] | Nd:YAG (sc) [10] |
|---|---|---|---|---|
| J–O parameters | $\Omega_2$ ($10^{-20}$ cm$^2$) | 0.224 | 0.220 | 0.200 |
| | $\Omega_4$ ($10^{-20}$ cm$^2$) | 2.567 | 3.550 | 2.700 |
| | $\Omega_6$ ($10^{-20}$ cm$^2$) | 3.712 | 5.330 | 5.000 |
| Spectroscopic quality factor | $X = \Omega_4/\Omega_6$ | 0.691 | 0.666 | 0.540 |
| Branching ratios | $\beta(^4F_{3/2} \rightarrow {}^4I_{9/2})$ | 0.379 | 0.409 | 0.370 |
| | $\beta(^4F_{3/2} \rightarrow {}^4I_{11/2})$ | 0.512 | 0.481 | 0.500 |
| | $\beta(^4F_{3/2} \rightarrow {}^4I_{13/2})$ | 0.104 | 0.108 | 0.130 |
| Radiative lifetime | $\tau(^4F_{3/2})$ (μs) | 316.0 | 238.0 | 250.0 |
| Quantum efficiency | $\eta$ (%) | 77.5 | 88.8 | 88.5 |

[a]This work.

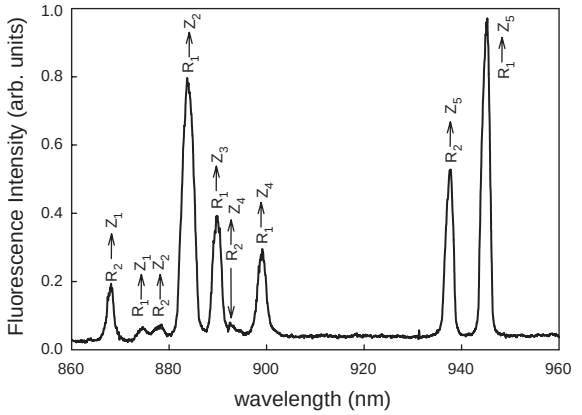


Fig. 1. Fluorescence spectrum of ceramic $Nd^{3+}$:YAG for $^4F_{3/2} \rightarrow {}^4I_{9/2}$ transition at 300 K.

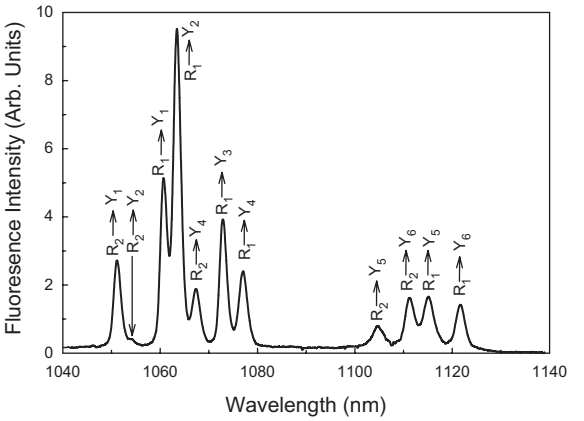


Fig. 2. Fluorescence spectrum of ceramic $Nd^{3+}$:YAG for $^4F_{3/2} \rightarrow {}^4I_{11/2}$ transition at 300 K.

emission line at 1063.5 nm in Fig. 2. This can be attributed to the large crystal field splitting of the $Nd^{3+}(4f^3)$ $^4F_{3/2}$ manifold in ceramic YAG.

The detailed characterization of the Stark energy levels of the $^4F_{3/2}$, $^4I_{9/2}$, and $^4I_{11/2}$ multiplets have been determined from the room temperature emission spectra for the $^4F_{3/2} \rightarrow {}^4I_{9/2}$ and $^4F_{3/2} \rightarrow {}^4I_{11/2}$ transitions of $Nd^{3+}(4f^3)$ in polycrystalline ceramic YAG. In order to determine the Stark energy level splitting of the upper manifold $^4F_{3/2}$, the emission spectra at 300 K were compared with those taken at 8 K as reported by Gruber et al. [9]. For example, there appeared only one peak at around 945 nm at 8 K due to the transition from the lower level of the $^4F_{3/2}$ manifold, while there are two peaks at around 945 and 938 nm due to transitions from both levels of the $^4F_{3/2}$ manifold state to the upper Stark level of the $^4I_{9/2}$ manifold; the difference between their positions provides the overall splitting of the $^4F_{3/2}$ manifold. The energy level diagram for the Stark components of the multiplet manifolds $^4F_{3/2}$, $^4I_{9/2}$, and $^4I_{11/2}$ is presented in Fig. 3. The arrows indicating the transitions $R_1 \rightarrow Z_5$ and $R_1 \rightarrow Y_2$ represent the emission peaks at 945.3 and 1063.5 nm in Figs. 1 and 2, respectively. These two transitions are the most intense ones and hence considered for determining the peak emission cross-sections. For

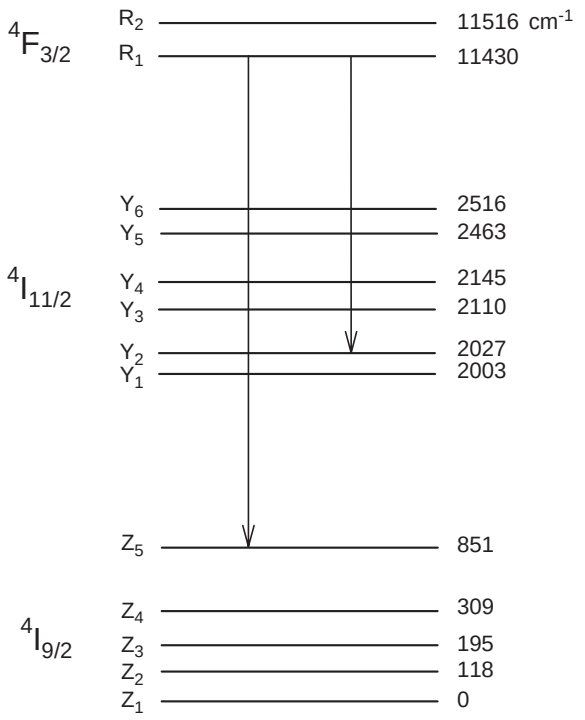


Fig. 3. Energy level diagram for the $^4F_{3/2}$, $^4I_{9/2}$ and $^4I_{11/2}$ multiplet manifolds of $Nd^{3+}$ in ceramic YAG at 300 K.

rare earth ions, the crystal field interaction splits the free-ion energy state of the manifold with total angular momentum of $J$ into $J+1/2$ levels for $J$ being half-odd integer. Therefore, the manifolds $^4F_{3/2}$, $^4I_{9/2}$, and $^4I_{11/2}$ are expected to split into 2, 5, and 6 Stark levels, respectively.

The peak emission cross-section is one of the most important parameters for the design of laser, because it describes the maximum spatial amplification of emission intensity. Since the line shapes for the inter-Stark transitions, $R_1 \rightarrow Z_5$ (945.3 nm) and $R_1 \rightarrow Y_2$ (1063.5 nm), of $Nd^{3+}(4f^3)$ in ceramic YAG host can be accurately fitted by a Gaussian line shape with the respective full-width at half-maximum (FWHM) of 16.4 and 16.1 cm$^{-1}$, the peak emission cross-sections ($\sigma_p$) for these transitions can be expressed accordingly in the following equations [10]:

$$\sigma_p(R_1 \rightarrow Z_5) = \frac{\lambda_p^2}{4\pi n^2 c \Delta\tilde{\nu}} \left[\frac{\ln 2}{\pi}\right]^{1/2} A(R_1 \rightarrow Z_5) \quad (1)$$

and

$$\sigma_p(R_1 \rightarrow Y_2) = \frac{\lambda_p^2}{4\pi n^2 c \Delta\tilde{\nu}} \left[\frac{\ln 2}{\pi}\right]^{1/2} A(R_1 \rightarrow Y_2), \quad (2)$$

where $\lambda_p$ is the wavelength at the peak position of the emission band, $c$ is the speed of light, and $\Delta\tilde{\nu}$ is the FWHM line width. The radiative probabilities of the inter-Stark transitions $R_1 \rightarrow Z_5$ and $R_1 \rightarrow Y_2$ can be expressed in the following respective equations [10]:

$$A(R_1 \rightarrow Z_5) = (1 + e^{-\Delta/kT})\beta(R_1 \rightarrow Z_5) \times \beta(^4F_{3/2} \rightarrow {}^4I_{9/2})\tau(^4F_{3/2})^{-1} \quad (3)$$

and

$$A(R_1 \rightarrow Y_2) = (1 + e^{-\Delta/kT})\beta(R_1 \rightarrow Y_2) \times \beta(^4F_{3/2} \rightarrow {}^4I_{11/2})\tau(^4F_{3/2})^{-1}, \quad (4)$$

where $\Delta$ is the difference in energy between the Stark levels $R_1$ and $R_2$ of the $^4F_{3/2}$ manifold, $k$ is the Boltzmann constant, $T$ is the absolute temperature, $\tau(^4F_{3/2})$ is the radiative lifetime of the $^4F_{3/2}$ metastable state, $\beta$ $(R_1 \rightarrow Z_5)$ and $\beta$ $(R_1 \rightarrow Y_2)$ represent the branching ratios for the corresponding inter-Stark transitions, and $\beta$ $(^4F_{3/2} \rightarrow {}^4I_{9/2})$ and $\beta$ $(^4F_{3/2} \rightarrow {}^4I_{11/2})$ are the branching ratios for the respective intermanifold transitions. The branching ratio for the inter-Stark transition is determined by comparing the area encompassed by the inter-Stark transition to the total area of the intermanifold transition. The analyses of Figs. 1 and 2 indicate that the $^4F_{3/2}$ manifold of ceramic $Nd^{3+}$:YAG is split into the Stark components $R_1$ and $R_2$ by 86 cm$^{-1}$. From the fluorescence data, we find $\beta$ $(R_1 \rightarrow Z_5) = 0.299$ and $\beta$ $(R_1 \rightarrow Y_2) = 0.279$. The constants $c$ and $k$ have their usual values. The index of refraction ($n$) is determined from the Sellmeier dispersion equation [7]:

$$n^2(\lambda) = 1 + \frac{2.2828\,\lambda^2}{\lambda^2 - 109.5856^2}. \quad (5)$$

Substituting the values for intermanifold and inter-Stark branching ratios and radiative lifetime from Table 1 along with the values of $\Delta$, $k$, and $T$, provide the inter-Stark radiative probabilities from Eqs. (3) and (4). These values and values of $\lambda_p$, $\Delta\tilde{\nu}$,

Table 2
Emission cross-sections of principal inter-Stark and intermanifold transitions of $Nd^{3+}$ ($4f^3$) in ceramic YAG

| | | |
|---|---|---|
| Emission cross-sections ($10^{-19}$ cm$^2$) | $\sigma(^4F_{3/2}\rightarrow{}^4I_{9/2})$ | 0.638 |
| | $\sigma(^4F_{3/2}\rightarrow{}^4I_{11/2})$ | 1.734 |
| | $\sigma_p(R_1\rightarrow Z_5)$ | 1.520 |
| | $\sigma_p(R_1\rightarrow Y_2)$ | 2.698 |

and $n$ are applied to Eqs. (1) and (2) to obtain the peak emission cross-sections of the inter-Stark transitions at 945.3 and 1063.5 nm. The values of these cross-sections are given in Table 2.

In addition, the emission cross-sections of the intermanifold transitions, $^4F_{3/2}\rightarrow{}^4I_{9/2}$ and $^4F_{3/2}\rightarrow{}^4I_{11/2}$ of $Nd^{3+}$($4f^3$) in polycrystalline ceramic YAG can be obtained using the following equation [11]:

$$\sigma(J,J';\tilde{\nu}) = \frac{\lambda^2}{8\pi cn^2}\frac{\beta(J,J')}{\tau_J}\,g(\tilde{\nu}), \tag{6}$$

where $\lambda$ is the peak emission wavelength and $\tilde{\nu}$ is the corresponding wave number, $\beta$ ($J$, $J'$) is the fluorescence branching ratio for the transition from the upper manifold $J$ to the lower manifold $J'$, $\tau_J$ is the radiative lifetime of the metastable manifold $J$ ($J = 3/2$), and $g(\tilde{\nu})$ is the line shape function. The line shape function is obtained from the fluorescence spectrum using the following expression [10]:

$$g(\tilde{\nu}) = \frac{I(\tilde{\nu})}{\int I(\tilde{\nu})\,d\tilde{\nu}}, \tag{7}$$

where $I(\tilde{\nu})$ is the intensity at $\tilde{\nu}$. The line shape functions for the $^4F_{3/2}\rightarrow{}^4I_{9/2}$ and $^4F_{3/2}\rightarrow{}^4I_{11/2}$ transitions can be therefore determined by dividing the peak intensities $I(\tilde{\nu})$ by the integrated areas of the respective fluorescence spectra. The values of $g(\tilde{\nu})$, along with the values of radiative lifetime and intermanifold branching ratios from Table 1, and the values of $\lambda$ and $n$ are applied to Eq. (7) to determine the emission cross-sections for the $^4F_{3/2}\rightarrow{}^4I_{9/2}$ and $^4F_{3/2}\rightarrow{}^4I_{11/2}$ intermanifold transitions; these values are given in Table 2.

## 4. Summary

A room temperature characterization of the Stark components of the $^4F_{3/2}$, $^4I_{9/2}$, and $^4I_{11/2}$ manifolds have been performed on the $Nd^{3+}$($4f^3$) $^4F_{3/2}\rightarrow{}^4I_{9/2}$ and $^4F_{3/2}\rightarrow{}^4I_{11/2}$ transitions in polycrystalline ceramic YAG. We have obtained the energy level separations of these transitions from both the low temperature and room temperature fluorescence spectra of ceramic $Nd^{3+}$:YAG. The accuracy of the arrangements of various Stark levels in the energy level diagram (Fig. 3) are found to be very good with an uncertainty of less than 2.0 cm$^{-1}$. The room temperature Stark level energies of $Nd^{3+}$ manifolds in ceramic YAG and the overall splitting of the manifolds are given in Table 3. These values are compared to those obtained by crystal-field modeling [9], and are found to be in good agreement. Nevertheless, it is important to mention that we have been able to clearly identify nine and eleven transitions in the room temperature fluorescence spectra due to the Stark component transitions within the $^4F_{3/2}\rightarrow{}^4I_{9/2}$ and $^4F_{3/2}\rightarrow{}^4I_{11/2}$ intermanifold transitions, respectively. One transition in the $^4F_{3/2}\rightarrow{}^4I_{9/2}$ spectrum has not been observed, and should have been located around 883.3 nm; the transition in the $^4F_{3/2}\rightarrow{}^4I_{11/2}$ spectrum is also not observed and would be located at about 1063.2 nm. The missing of these two peaks due to the inter-Stark transitions in the respective manifolds could be attributed to the lack of spectral resolution of the instrument that is only 0.8 nm.

The inter-Stark emissions at 945.3 and 1063.5 nm are found to possess the Gaussian line shape; this is indicative of inhomogeneous broadening. The peak emission cross-sections of these inter-Stark transitions and the emission cross-sections of the $^4F_{3/2}\rightarrow{}^4I_{9/2}$ and $^4F_{3/2}\rightarrow{}^4I_{11/2}$ intermanifold transitions have also been determined. The emission cross-section of the most popular transition, $^4F_{3/2}\rightarrow{}^4I_{11/2}$, for ceramic $Nd^{3+}$:YAG is $1.73\times10^{-19}$ cm$^2$ and that of $Nd^{3+}$:YAG single crystal [10] is $2.80\times10^{-19}$ cm$^2$. These values are agreeable within the experimental uncertainties. It is also important to note that the spectroscopic parameters of ceramic $Nd^{3+}$:YAG, determined by the J–O theoretical model are found to be quite similar to those of single-crystal $Nd^{3+}$:YAG [7].

In conclusion, our current and previous studies show that ceramic $Nd^{3+}$:YAG possesses several

Table 3
Stark level energies of $Nd^{3+}$ in ceramic YAG and total manifold splitting

| $Nd^{3+}$ multiplet | Energy[a] ($cm^{-1}$) | Overall splitting[a] ($cm^{-1}$) | Energy ($cm^{-1}$) [9] | Overall splitting ($cm^{-1}$) [9] |
|---|---|---|---|---|
| $^4F_{3/2}$ | 11516 | 86 | 11508 | 83 |
| | 11430 | | 11425 | |
| $^4I_{11/2}$ | 2516 | 513 | 2520 | 517 |
| | 2463 | | 2470 | |
| | 2145 | | 2146 | |
| | 2110 | | 2110 | |
| | 2027 | | 2030 | |
| | 2003 | | 2003 | |
| $^4I_{9/2}$ | 851 | 851 | 860 | 860 |
| | 309 | | 310 | |
| | 195 | | 200 | |
| | 118 | | 131 | |
| | 0 | | 0 | |

[a]This work.

competitive spectroscopic properties suggesting that this material has potential for laser operations in near infrared region. In particular, owing to the higher branching ratio of the $^4F_{3/2} \rightarrow {}^4I_{11/2}$ inter-manifold transition [7] and the suitable emission cross-section of the $R_1 \rightarrow Y_2$ inter-Stark transition, ceramic $Nd^{3+}$:YAG could be an excellent candidate for a 1.06 μm laser.

## Acknowledgments

This research was supported by the National Science Foundation Grant No. DMR-0099479. The authors would like to thank Charles Russell for taking some room temperature absorption and emission spectra.

## References

[1] M. Sekita, H. Haneda, Y. Yanagitani, S. Shirasaki, J. Appl. Phys. 67 (1990) 453.
[2] C. Greskovich, J.P. Chernoch, J. Appl. Phys. 44 (1973) 4599.
[3] J. Lu, M. Prabhu, J. Xu, K. Ueda, H. Yagi, T. Yanagitani, A.A. Kaminskii, Appl. Phys. Lett. 77 (2000) 3707.
[4] J. Lu, K. Ueda, H. Yagi, T. Yanagitani, Y. Akiyama, A.A. Kaminskii, Appl. Phys. Lett. 77 (2000) 3707.
[5] A.A. Kaminskii, M.Sh. Akcharia, V.I. Alahita, K. Ueda, K. Takachi, J. Lu, T. Uematsu, M. Musha, A. Shirikawa, V. Gabler, H.J. Eichler, H. Yagi, T. Yamagitani, S.N. Bagayev, J. Fernandes, R. Baldu, Quantum Electronics Conference, IQEC-2002, June 22–27, 2002, Moscow.
[6] G.A. Kumar, J. Lu, A.A. Kaminskii, K. Ueda, H. Yagi, T. Yanagitani, N.V. Unnikrishnan, IEEE J. Quantum Electron. 40 (2004) 747.
[7] D.K. Sardar, C.C. Russell, J.B. Gruber, T.H. Allik, J. Appl. Phys. 97 (2005) 123501.
[8] Baikowski International Corp., Ceramic YAG Specifications, for Konoshima Chemical Industry KK, Japan, 2003.
[9] J.B. Gruber, D.K. Sardar, R.M. Yow, T.H. Allik, B. Zandi, J. Appl. Phys. 96 (2004) 3050.
[10] W.F. Krupke, M.D. Shinn, J.E. Marion, J.A. Caird, S.E. Stokowski, J. Opt. Soc. Am. B. 3 (1986) 102.
[11] W. Koechner, in: H.K.V. Lotsch, Solid-State Laser Engineering, Springer Series in Optical Sciences, vol. 1, fourth ed., Springer, Berlin, 1996, p. 15.